

Coordinated Intra- and Inter-system Interference Management in Integrated Satellite Terrestrial Networks

Ziyue Zhang, Min Sheng, *Senior Member, IEEE*, Junyu Liu, *Member, IEEE*, and Jiandong Li, *Fellow, IEEE*

State Key Laboratory of Integrated Service Networks, Xidian University, Xi'an, Shaanxi, 710071, China
Email: zhangziyue@stu.xidian.edu.cn, msheng@mail.xidian.edu.cn, junyuliu@xidian.edu.cn, jdli@mail.xidian.edu.cn

Abstract

Leveraging the advantage of satellite and terrestrial networks, the integrated satellite terrestrial networks (ISTNs) can help to achieve seamless global access and eliminate the digital divide. However, the dense deployment and frequent handover of satellites aggravate intra- and inter-system interference, resulting in a decrease in downlink sum rate. To address this issue, we propose a coordinated intra- and inter-system interference management algorithm for ISTN. This algorithm coordinates multidimensional interference through a joint design of inter-satellite handover and resource allocation method. On the one hand, we take inter-system interference between low earth orbit (LEO) and geostationary orbit (GEO) satellites as a constraint, and reduce interference to GEO satellite ground stations (GEO-GS) while ensuring system capacity through inter-satellite handover. On the other hand, satellite and terrestrial resource allocation schemes are designed based on the matching idea, and channel gain and interference to other channels are considered during the matching process to coordinate co-channel interference. In order to avoid too many unnecessary handovers, we consider handover scenarios related to service capabilities and service time to determine the optimal handover target satellite. Numerical results show that the gap between the results on the system sum rate obtained by the proposed method and the upper bound is reduced as the user density increases, and the handover frequency can be significantly reduced.

Index Terms

Integrated satellite terrestrial networks, inter-satellite handover, intra- and inter-system interference management.

I. INTRODUCTION

In the emerging 6th generation (6G) wireless communication networks, the integrated satellite terrestrial networks (ISTNs) can provide expanded coverage and seamless connectivity [1]–[3]. ISTNs offer wide signal coverage for ground users (GUs) in remote areas and high-quality services for hotspots while ensuring communication quality [4]–[6]. However, the co-channel interference in the ISTN and the collinear interference between geostationary (GEO) and low earth orbit (LEO) satellites degrades the downlink rate of ISTNs. With the increasing number of deployed LEO satellites, intra-system co-channel and inter-system collinear interference is further aggravated. Moreover, the fast movement of LEO satellites makes the inter-satellite handover occur frequently, which makes the interference management problem more complex. Therefore, an effective handover strategy is required to mitigate interference and optimize resource allocation. Considering the synergy between intra- and inter-system interference, it is necessary to manage the intra- and inter-system interference in ISTN through the inter-satellite handover and resource allocation.

A. Related work

In ISTN, intra-system interference management has been extensively investigated. The design of the resource allocation method for power and spectrum is essential for interference management in ISTN [7]–[11]. To reduce intra-system interference, a dynamic power allocation algorithm suitable for satellites operating in the Ka-band was proposed in [7]. However, the influence of cloud and rain decline was not considered, resulting in an inaccurate description of the interference. Furthermore, an optimal bandwidth constraint was proposed in [8], which reduced intra- and inter-beam interference by optimizing frequency bandwidth and power allocation. In the emerging 6th generation (6G) wireless communication networks, the integrated satellite terrestrial networks (ISTNs) can provide expanded coverage and seamless connectivity [1], [2]. ISTNs offer wide signal coverage for ground users (GUs) in remote areas and high-quality services for hotspots while ensuring communication quality [4], [5]. However, the co-channel interference in the ISTN and the collinear interference between geostationary (GEO) and low earth orbit (LEO) satellites degrades the downlink rate of ISTNs. With the increasing number of deployed LEO satellites, intra-system

Ziyue Zhang, Junyu Liu, Min Sheng, and Jiandong Li are with the State Key Laboratory of Integrated Service Networks, Xidian University, Xi'an, Shaanxi, 710071, China. (e-mail: zhangziyue@xidian.edu.cn; junyuliu@xidian.edu.cn; {msheng, jdli}@mail.xidian.edu.cn).

(Corresponding author: Junyu Liu.)

co-channel and inter-system collinear interference is further aggravated. Moreover, the fast movement of LEO satellites makes the inter-satellite handover occur frequently, which makes the interference management problem more complex. Then, the scenario of co-frequency interference in ISTN was first analyzed in [9]. Simulation results illustrate that dynamic resource allocation could effectively reduce intra-system interference compared to fixed resource allocation. A resource allocation scheme with interference cooperation was proposed in [10], in which the original problem was divided into three stages to be solved sequentially. Although the above researches can effectively alleviate intra-system interference, with the intensive deployment of LEO satellites, the collinear interference between LEO and GEO satellites needs to be considered.

For inter-system interference in ISTN, power allocation and spatial isolation can be employed to avoid interference [12]–[16]. In [12], a collinear interference suppression method for GEO and LEO satellite spectrum sharing was proposed. Collinear interference is mitigated by optimizing the transmit power of the satellites. In addition, a cognitive distance power control scheme was proposed to avoid the interference of LEO satellites to GEO satellites by controlling the distance between satellite system terminals [13]. In [14], interference caused by the operation of the LEO system uplink and downlink on the GEO system was analyzed, and a method of avoiding interference by setting an exclusion angle was proposed in [15], respectively. Based on the above analysis of interference, a power control technique was proposed to increase the downlink rate under the GEO quality of service (QoS) constraint in [16]. However, the existing power control methods compromise the system capacity, and spatial isolation comes at the cost of communication quality.

The highly dynamic nature of the network topology results in frequent handovers between terrestrial terminals and satellites, which also leads to a decrease in the performance of ISTN [17]. Inter-satellite handover is considered as an effective solution for inter-system interference and resource allocation in ISTN [18]–[20]. In [18], a weighted bipartite graph based handover strategy was proposed for the links between the satellites and gateway stations. The channel gain is used as the handover weight. However, inter-satellite handover would change the LEO satellites that can be connected by TBSs, which may affect the distribution of co-channel interference and degrade the backhaul capacity. Therefore, matching games have been introduced to solve the problem of co-channel interference management in ISTN [21]–[25]. A game matching based resource allocation method was proposed to improve the transmission rate in [21]. In addition, a dynamic spectrum partitioning strategy was proposed to mitigate interlayer interference in [24]. Through the matching process, both interference mitigation and user fairness can be considered, and the downlink sum rate can be improved.

Despite the extensive literature on intra- and inter-system interference management in ISTN, most existing studies ignore the combined impact of intra- and inter-system interference on system capacity. The dense distribution of LEO satellites leads to aggravated inter-system interference, which may reduce the system capacity and affect the intensity of intra-system co-channel interference. For comprehensive management of complex interference in ISTNs, it is necessary to develop a unified framework to effectively integrate interference management at intra- and inter-system levels, which could capture the effect of inter-system interference on system capacity and facilitate the coordinated management of intra-system co-channel interference.

B. Contribution

In this paper, a coordinated intra- and inter-system interference management (CIIM) algorithm is proposed for ISTN. CIIM leverages the correlation of intra- and inter-system interference to conduct coordination between the LEO and GEO satellites system, and coordination of intra-system interference in ISTN through resource allocation. The main contributions of this paper are summarized as follows.

- For inter-system collinear interference, an interference management algorithm based on inter-satellite handover is proposed. The algorithm enables the handover of LEO satellites through the working threshold to avoid collinear interference. Since frequent handovers will lead to a decline in real-time decision making, we introduce a handover threshold based on the signal strength difference to remove LEO satellites that cannot meet the handover conditions. By adjusting the handover threshold, the trade-off between capacity improvement and handover frequency can be balanced.
- To coordinate intra-system co-channel interference, we propose a user association and resource allocation method based on game matching. During the matching process, GUs are inclined to select subchannels with high channel power gain and low co-channel interference. Moreover, TBSs dynamically adjust power allocation according to user distribution and channel conditions to reduce interference to other GUs. With the increasing user density, we show via simulation results that the gap between the results on the system sum rate obtained by the proposed method and the upper bound is reduced.

The remainder of this paper is organized as follows. Firstly, the system model is introduced in Section II. In Section III, the intra- and inter-system interference management problem is formulated and decomposed into two subproblems. Then, the CIIM scheme is detailed in Section IV. In Section V, the proposed algorithms are evaluated through simulations. The paper concludes in Section VI.

II. SYSTEM MODEL

In this section, the ISTN model is briefly introduced. Then the cached model, terrestrial transmission model and satellite transmission model are given. The notations and definitions used in this paper are shown in Tab I.

Table I
NOTATIONS AND DEFINITIONS

Notations	Definitions
$\mathcal{M}, \mathcal{J}, \mathcal{N}, \mathcal{L}$	Sets of TBSs, GUs and LEO satellites.
M, J, N, L	Number of TBSs, GUs and LEO satellites.
\mathcal{C}, \mathcal{K}	Sets of subchannels available for TBSs and LEO satellites.
N_C, N_K	Number of subchannels available for TBSs and LEO satellites.
G_T, G_R	Gain of the transmit and the receive antennas.
p_{leo}	The transmit power of LEO satellites.
B_C, B_{Ka}	The bandwidth of C-band and Ka-band.

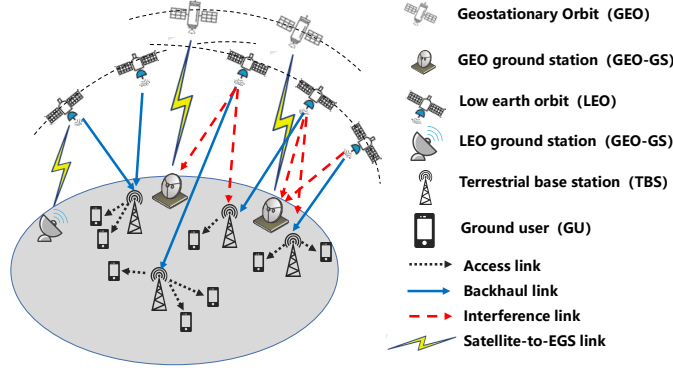


Fig. 1. System model of downlink ISTNs.

A. Network Model

We consider a downlink communication scenario of ISTN in Fig. 1, where M TBSs and N LEO satellites are deployed to provide service to J GUs. In addition, there are L GEO satellite ground stations (GEO-GSs) distributed in this area. The GEO satellite and LEO satellites share the same frequency band to serve the GEO-GSs and TBSs, respectively. The sets of GEO-GSs, TBSs and GUs are denoted by $\mathcal{L} = \{1, \dots, l, \dots, L\}$, $\mathcal{M} = \{1, \dots, m, \dots, M\}$ and $\mathcal{J} = \{1, \dots, j, \dots, J\}$, while the set of LEO satellite is denoted as $\mathcal{N} = \{1, \dots, n, \dots, N\}$. In ISTN, TBSs can store popular content for data offloading, enabling GUs to access the network through the available subchannels (SCs) of their associated TBSs. LEO satellites provide backhaul service to GUs through TBSs [21]. Each TBS carries multiple independent antennas to establish connections with multiple LEO satellites simultaneously [26]. Let $\mathcal{T} = \{1, \dots, t, \dots, T\}$ denote the set of timeslots (TSs). We assume that channel state information (CSI) between LEO satellites and TBSs is known at all timeslots.

We define the C-band and Ka-band bandwidth as B_C and B_{Ka} , respectively. To achieve higher transmission rate, full frequency reuse is considered and the co-channel interference cannot be ignored. The main types of interference in ISTN include intra-system co-channel interference and inter-system collinear interference between LEO and GEO satellites.

B. Caching Model

The local caching capability enables data offloading and traffic splitting, which reduces network backhaul pressure [10]. Through caching files at TBSs, wireless caching enables GUs to download the requested files directly from the TBSs' local storage, thereby reducing the traffic overhead and communication time. Let $\mathcal{F} = \{1, \dots, f, \dots, F\}$ denote the set of requested files, which contains F files. The content popularity vector is denoted by $Q = \{q_f \mid f = 1, 2, \dots, F\}$, where q_f represents the popularity of the file f . The content popularity q_n follows the Zipf distribution [27], which is expressed as

$$q_f = \frac{f^{-\omega}}{\Omega}, \quad \forall f \in \mathcal{F}, \quad (1)$$

where $\sum_{f=1}^F q_f = 1$ and ω is the Zipf distribution index. Files with high popularity are always requested, so popularity can also be used as the probability of GU request. To represent the caching status of the TBSs, we define a binary matrix $G[g_{m,j}]_{M \times J}$, where $g_{m,j} = 1$ indicates that TBS m caches the file requested by GU j , and $g_{m,j} = 0$ otherwise. It is assumed that all TBSs have the same caching capacity. To efficiently use the caching capability of the TBS, each GU is allowed to request only one file from the associated TBS at one TS.

C. Terrestrial Transmission Model

In the terrestrial network, each GU associates to the TBS that provides the maximum average received power [28]. Each TBS can serve multiple GUs while each GU can be associated to only one TBS. We define an indicator variable $a_{m,j}^t$ to describe the connection relationship between GUs and TBSs, where $a_{m,j}^t = 1$ represents that GU j is served by TBS m in TS t , and $a_{m,j}^t = 0$ otherwise. The set of available SCs of the TBS is denoted by $\mathcal{C} = \{1, \dots, c, \dots, C\}$. For GUs, we define a binary matrix $X[x_{m,j,c}^t]_{M \times J \times C}$ to describe their groups, where $x_{m,j,c} = 1$ represents that GU j is served by TBS m over SC c in TS t and $x_{m,j,c} = 0$, otherwise. Let $P[p_{m,j,c}^t]_{M \times J \times C}$ denote the transmit power from TBS m to GU j over SC c in TS t . Thus, the received signal of GU j in TS t is given by

$$y_{m,j}^t = \sum_{m \in M} \sum_{j_i \in J} \sqrt{p_{m,j_i,c}^t} h_{m,j,c} u_{m,j_i,c} + N_m, \quad (2)$$

where $h_{m,j,c}$ is the channel gain from TBS m to GU j , $u_{m,j_i,c}$ represents the transmit signal from TBS m to GU j_i over SC c and N_m represents the additive white Gaussian Noise (AWGN) at TBS m . Thus, the Signal-interference-noise Ratio (SINR) of a GU j is obtained by

$$\gamma_{m,j,c}^t = \frac{p_{m,j,c}^t x_{m,j,c}^t |h_{m,j,c}|^2}{\underbrace{\sum_{m_i \neq m} \sum_{j_i \neq j} p_{m_i,j_i,c}^t x_{m_i,j_i,c}^t |h_{m_i,j_i,c}|^2}_{\text{Intra-system co-channel interference}} + \sigma_n^2}, \quad (3)$$

where σ_n^2 is the AWGN power. Therefore, the transmission rate of GU j from TBS m on SC c is calculated as

$$R_{m,j,c}^t = B_C \log_2 (1 + \gamma_{m,j,c}^t). \quad (4)$$

Note that GU's transmission rate is constrained by the backhaul traffic. When the GUs request files from LEO satellites through associated TBSs, it is assumed that each download will generate the same traffic, denoted as U_{back} . Therefore, the achievable transmission rate of GU j that needs to request files from the LEO satellite is reformulated as

$$R_{m,j,c}^t = \min_{(g_{m,j}=0)} (R_{m,j,c}^t, U_{\text{back}}). \quad (5)$$

D. LEO Backhaul Transmission Model

We assume that fixed spatial positions for LEO satellites at each TS. We denote the set of available SCs of the LEO satellites by $\mathcal{K} = \{1, \dots, k, \dots, K\}$. In ISTN, TBSs are under multiple satellite coverage, and each TBS can be served by N_r satellites simultaneously. Due to the movement of LEO satellites, TBSs need to switch to other satellites to ensure service continuity. A binary matrix $B[b_{n,m,k}^t]_{N \times M \times K}$ is provided to represent the relationship between LEO satellites and TBSs, where $b_{n,m,k}^t = 1$ indicates that TBS m is served by LEO satellite n over SC k in TS t . The elevation angle between LEO satellite n and TBS m at TS t can be expressed as $\theta_{n,m}^t$, which can be calculated from the satellite position information predicted by the TBSs. The transmission rate of GUs is limited by LEO-TBS backhaul links. Specifically, the backhaul traffic consumed by GUs requesting files cannot exceed the backhaul capacity of TBSs. Accordingly, the backhaul SINR of TBS m from LEO satellite n is calculated as

$$\gamma_{n,m,k}^t = \frac{b_{n,m,k}^t p_{n,m,k}^t h_{n,m,k}}{\underbrace{\sum_{n_i \neq n} \sum_{m_i \neq m} b_{n_i,m_i,k}^t p_{n_i,m_i,k}^t h_{n_i,m_i,k}}_{\text{Inter-satellite co-channel interference}} + \sigma_n^2}, \quad (6)$$

where $p_{n,m,k}^t$ is the transmit power allocated to TBS m by LEO satellite n over SC k in TS t and $h_{n,m,k}$ is the channel gain from LEO satellite n to TBS m . And the backhaul rate of TBS m from LEO satellite n is expressed as

$$R_{n,m,k}^t = B_{\text{Ka}} \log_2 (1 + \gamma_{n,m,k}^t), \quad (7)$$

Thus, the backhaul capacity of TBS m is obtained

$$C_m^t = \sum_{n \in N} \sum_{k \in K} R_{n,m,k}^t. \quad (8)$$

The downlink from the LEO satellites can potentially cause interference to GEO-GS [12]. For the GEO-GS l , the interference caused by LEO satellites at TS t is given by

$$I_l^t = \sum_{n \in \mathcal{N}} \sum_{m \in \mathcal{M}} b_{n,m,k}^t p_{n,m,k}^t h_{n,l}, \quad (9)$$

where $h_{n,l}$ is the channel gain from LEO satellite n to the GEO-GS l .

III. PROBLEM FORMULATION AND DECOMPOSITION

This section models a system sum rate maximization problem that satisfies the inter-system interference constraint. Then the original problem is decomposed into two subproblems to be solved.

A. Problem Formulation

In ISTN, a high transmission rate of GU is expected to be conducted. However, intra- and inter-system interference may limit the LEO backhaul capacity and affect the transmission rate of GUs [29]. Therefore, the goal of interference management is to maximize the system sum rate while ensuring that each GEO-GS satisfies the interference constraints. Accordingly, the intra- and inter-system interference management problem is formulated as

$$\max_{\{X,B,P\}} \sum_{m \in \mathcal{M}} \sum_{j \in \mathcal{J}} \sum_{c \in \mathcal{C}} R_{m,j,c}^t \quad (10)$$

$$s.t. \text{C1} : x_{m,j,c}^t \leq a_{m,j}^t, \forall m \in \mathcal{M}, \forall j \in \mathcal{J}, \forall t \in \mathcal{T}, \quad (11a)$$

$$\text{C2} : \sum_{m \in \mathcal{M}} \sum_{c \in \mathcal{C}} x_{m,j,c}^t \leq 1, \forall j \in \mathcal{J}, \forall t \in \mathcal{T}, \quad (11b)$$

$$\text{C3} : \sum_{j \in \mathcal{J}} x_{m,j,c}^t \leq 1, \forall m \in \mathcal{M}, \forall c \in \mathcal{C}, \forall t \in \mathcal{T}, \quad (11c)$$

$$\text{C4} : \theta_{n,m}^t \geq \theta_{min}, \forall n \in \mathcal{N}, \forall m \in \mathcal{M}, \forall t \in \mathcal{T}, \quad (11d)$$

$$\text{C5} : \sum_{n \in \mathcal{N}} \sum_{k \in \mathcal{K}} b_{n,m,k}^t \leq N_r, \forall m \in \mathcal{M}, \forall t \in \mathcal{T}, \quad (11e)$$

$$\text{C6} : \sum_{m \in \mathcal{M}} b_{n,m,k}^t \leq 1, \forall n \in \mathcal{N}, \forall k \in \mathcal{K}, \forall t \in \mathcal{T}, \quad (11f)$$

$$\text{C7} : \sum_{j \in \mathcal{J}} \sum_{c \in \mathcal{C}} x_{m,j,c}^t (1 - g_{m,j}) U_{back} \leq C_m^t, \forall m \in \mathcal{M}, \forall t \in \mathcal{T}, \quad (11g)$$

$$\text{C8} : \sum_{j \in \mathcal{J}} \sum_{c \in \mathcal{C}} x_{m,j,c}^t p_{m,j,c}^t \leq P_{TBS}, \forall m \in \mathcal{M}, \forall t \in \mathcal{T}, \quad (11h)$$

$$\text{C9} : I_l^t \leq I_{th}, \forall t \in \mathcal{T}. \quad (11i)$$

C1 indicates that each GU is associated with only one TBS, while C2 and C3 restrict the number of SCs assigned to each GU and the number of GUs assigned to each SC, respectively. C4 constrains the selection range of target LEO satellites for each TBS. C5 and C6 indicate that each TBS can be served by N_r satellites simultaneously. The backhaul link constraint in ISTN is represented by C7, while C8 ensures that the power allocated to each SC is within the maximum power of the TBS. Finally, C9 denotes that the interference to GEO-GS should meet the maximum interference threshold I_{th} requirements.

The optimization problem (10) is a non-convex integer nonlinear programming problem with NP complexity. Due to the backhaul link constraint, a direct transformation of problem (10) into a convex optimization problem is difficult. To address this, we adopt the Lagrangian dual method to decompose the original problem (10) into two subproblems, enabling us to obtain the solution more efficiently. Note that the result obtained in this way does not always satisfy the backhaul link constraint C7, so we reduce GUs accessing the TBSs to ensure that the consumed backhaul traffic does not exceed the backhaul capacity.

B. Problem Decomposition

Due to the fact that the backhaul link constraint is considered in the model, this optimization problem (10) is not convex. Hence, we consider the dual problem of the original problem. By introducing non-negative Lagrangian multiplier λ , the dual optimum of the problem in (10) is expressed as

$$d^* = \min_{\lambda \geq 0} d(\lambda) \triangleq \min_{\lambda \geq 0} \max_{\{X,B,P\}} \mathcal{L}(X, B, P, \lambda), \quad (11)$$

where $\lambda = \{\lambda_1, \lambda_2, \dots, \lambda_M\}$.

Thus, the Lagrange function is defined as

$$\begin{aligned}
\mathcal{L}(X, B, P, \lambda) &= \sum_{m \in \mathcal{M}} \sum_{j \in \mathcal{J}} \sum_{c \in \mathcal{C}} R_{m,j,c} \\
&+ \sum_{m \in \mathcal{M}} \lambda_m \left(C_m - \sum_{j \in \mathcal{J}} \sum_{c \in \mathcal{C}} x_{m,j,c} (1 - g_{m,j}) U_{\text{back}} \right) \\
&= \sum_{m \in \mathcal{M}} \sum_{j \in \mathcal{J}} \sum_{c \in \mathcal{C}} R_{m,j,c} \\
&- \sum_{m \in \mathcal{M}} \lambda_m \sum_{j \in \mathcal{J}} \sum_{c \in \mathcal{C}} x_{m,j,c} (1 - g_{m,j}) U_{\text{back}} \\
&+ \sum_{m \in \mathcal{M}} \lambda_m C_m.
\end{aligned} \tag{12}$$

Proposition 1. Assume that $f(x)$ and $d(\lambda)$ are the primary problem and dual problem. In addition, $f_m(x)$ are the relaxed constraints. The Lagrange multiplier is denoted by λ . The optimal solutions of the primary problem and dual problem are denoted by f^* and d^* , respectively. The d^* obtained is an upper bound to the optimal solution f_0^* .

Proof: The Lagrange function is expressed as

$$\mathcal{L}(x, \lambda) = f(x) + \sum_{m \in \mathcal{M}} \lambda_m f_m(x), \tag{13}$$

Let \dot{x} be an arbitrary point within the feasible domain \mathcal{D} of the primary problem. The corresponding dual function (11) is denoted by

$$\begin{aligned}
d(\lambda) &= f(\dot{x}) + \sum_{m \in \mathcal{M}} (\lambda_m f_m(\dot{x})) \\
&\geq f(\dot{x}).
\end{aligned} \tag{14}$$

We observe that (14) holds for any points \mathcal{D} . Accordingly, the dual optimum is an upper bound to the optimal solution of primary problem, expressed as

$$d^* \geq f^*, \tag{15}$$

where f_0^* and d^* are the optimal solutions of primary problem and dual problem. \square

Note that d^* is an upper bound of primary problem (10), as stated in Proposition 1. We observe that (12) is determined by X , B and P . Thus, the primary problem is decomposed into the following two subproblems.

The inter-satellite interference and handover management subproblem is given by

$$\begin{aligned}
\mathbf{P1} : \max_{\{B\}} & \sum_{m \in \mathcal{M}} \lambda_m C_m \\
& s.t. \text{ C4-C9}.
\end{aligned} \tag{16}$$

The goal of P1 is to maximize the backhaul capacity through the management of inter-satellite interference while satisfying the constraints of inter-system interference. Considering that TBSs can connect to multiple LEO satellites simultaneously, P1 can be transformed into a many-to-one matching problem. It is noted that the inter-system interference constraint C9, which helps to reduce the feasible region of resource allocation.

The terrestrial resource allocation subproblem is formulated as

$$\begin{aligned}
\mathbf{P2} : \max_{\{X, P\}} & \sum_{m \in \mathcal{M}} \sum_{j \in \mathcal{J}} \sum_{c \in \mathcal{C}} R_{m,j,c} \\
& - \sum_{m \in \mathcal{M}} \lambda_m \sum_{j \in \mathcal{J}} \sum_{c \in \mathcal{C}} x_{m,j,c} (1 - g_{m,j}) U_{\text{back}} \\
& s.t. \text{ C1-C3, C7}.
\end{aligned} \tag{17}$$

P2 aims at maximizing the system sum rate under the backhaul link constraint by coordinating intra-system interference. To achieve this goal, the GUs are classified into backhaul-GUs and local-GUs according to file request status and cache status. Specifically, when the file requested by the GU is cached by its associated TBS, denoted by $g_{m,j} = 1$, the GU is classified as a local-GU, otherwise, as a backhaul-GU. We find that P2 can be divided into two parts: subchannel allocation and power allocation. SC allocation problem can be transformed into a one-to-one matching problem, and then we find a feasible solution for the power allocation by the water injection power algorithm.

IV. COORDINATED INTRA- AND INTER-SYSTEM INTERFERENCE MANAGEMENT METHOD DESIGN

In this section, we first specifically describe the interaction between resource allocation and handover, and propose interference management combined with inter-satellite handover algorithm to optimize the allocation and handover selection in each TS. Subsequently, we design a user association and resource allocation algorithm to optimize the downlink sum rate of the entire ISTN while satisfying satellite-terrestrial constraint. Finally, we introduce a coordinated intra- and inter-system method and analyze its convergence and complexity.

A. Interference Management combined with Inter-Satellite Handover

As presented in (16), the satellite interference and handover management problem is compounded by the dense deployment of LEO satellites, which results in inter-satellite interference, inter-system collinear interference and frequent inter-satellite handover. Considering that TBSs can be served by multiple LEO satellites, P1 can be reformulated as a many-to-one matching problem subject to the inter-system constraint [30]. After the inter-system interference constraint is satisfied through inter-satellite handover, multiple LEO satellites are matched with a single TBS to improve the backhaul capacity. Specifically, if the CINR of the GEO-GS is lower than the interference threshold I_{th} , the inter-satellite handover is guided according to the received signal strength, and the TBS will connect to the LEO satellite with less interference to avoid inter-system interference.

1) *Preparation process*: Define Φ is the mapping of the set $\{\mathcal{M} \cup \mathcal{N} \cup \mathcal{K}\}$. To jointly consider LEO satellites and SCs, we use (l, k) to represent the LEO-SC unit. The goal of a matching Φ is to obtain a stable $(m, (n, k))$ matching pair.

2) *Preference relationship*: To eliminate TBS-satellite interference, SIC is introduced in the matching process. Considering the order of SIC decoding, the preference of TBS-satellite-SC unit $(m, (n, k))$ is denoted by

$$\rho_{m,(n,k)}^{m',(n',k)} = \begin{cases} |h_{n',m',k}|^2 / |h_{n,m,k}|^2, & h_{n',m',k} > h_{n,m,k}, \\ |h_{n',m',k}|^2, & h_{n',m',k} \leq h_{n,m,k}. \end{cases} \quad (18)$$

If $\rho_{m,(s_1,k)}^{m_1,(s_1,k)} > \rho_{m,(s_2,k)}^{m_2,(s_2,k)}$, the matched pair is more likely to be updated as $(m_1, (s_1, k))$ rather than $(m_2, (s_2, k))$.

3) *Matching process*: Initially, we sorted the TBS-satellite units in descending order of preference and each SC is matched in order. Specifically, to balance the quality and quantity of TBS-satellite links, unmatched TBSs select the worst link satisfying

$$m^*, (n^*, k) = \arg \max_{m \in \mathcal{M}_{un}} \min_{n \in \mathcal{N}_{un,k}} h_{n,m,k}. \quad (19)$$

In (19), \mathcal{M}_{un} is the set of TBSs connected to fewer than N_r satellites. $\mathcal{N}_{un,k}$ is the set of unmatched LEO satellites over SC k .

Considering the co-channel interference between matching pairs, we allow potential matching pairs to accept the proposal of matched unit (m, n) , and candidate matching pairs are defined as follows

$$(m', n') = \arg \max_{m' \in \mathcal{M}_{un}, n' \in \mathcal{N}_{un,k}} \rho_{m,(n,k)}^{m',(n',k)}, \quad (20)$$

$$(m', n'_g) = \arg \max_{m' \in \mathcal{M}_{un}, n'_g \in \mathcal{N}_{un,k}^g} \rho_{m,(n,k)}^{m',(n'_g,k)}. \quad (21)$$

In (20) and (21), $\mathcal{N}_{un,k}^g$ is the set of LEO satellites whose channel gain is greater than that of the matching pair $(m, (n, k))$, so that co-channel interference between matching pairs can be avoided by introducing SIC. The set \mathcal{T} consists of candidate matching pairs $(m', (n', k))$ and $(m', (n'_g, k))$.

4) *Handover process*: The interference of GEO-GS is calculated according to (19). If the value is lower than I_{th} , the interference caused by the LEO satellites in each visible range is calculated according to the received signal power of GEO-GS. For a TBS, when the difference between the received signal strength and interference signal of other LEO satellites is higher than the currently connected LEO satellite, it will choose the satellite with less interference to connect. Therefore, we define a handover utility function, which is represented by the difference between the received signal strength of TBS and the interference signal strength of GEO-GS. The larger the utility function, the greater the benefit of handover the TBS to a new LEO satellite, which can reduce the interference to GEO satellites. The handover utility is denoted by

$$U_n = \sum_{m=1}^{N_M} \sum_{k=1}^{N_K} b_{n,m,k} p_{n,m,k} h_{n,m,k} - \sum_{m=1}^{N_M} \sum_{k=1}^{N_K} b_{n,m,k} p_{n,m,k} h_{n,g} \quad (22)$$

To reduce the handover frequency and increase the handover gain, a threshold H is set. When the handover utility of a new LEO satellite n exceeds the threshold H , the handover is triggered. After the original satellite is switched to the new satellite, the new satellites will provide backhaul services to TBSs to respond to user requests. Then, update the candidates in \mathcal{T} and

proceed with further matching. The utility of SC k is set as the sum transmission rate achieved by all TBSs over it. Then, each SC chooses a candidate matching pair $(m'', (n'', k))$ based on the utility, expressed as

$$\mathcal{R}_m = \sum_{m=1}^{N_M} \lambda_m C_m. \quad (23)$$

Thus, the matching rules is defined as

$$\Phi_1 \succ_k \Phi_2 \Leftrightarrow \mathcal{R}_k(\Phi_1) > \mathcal{R}_k(\Phi_2). \quad (24)$$

If a TBS receives proposals from more than N_r SCs, it sorts these units in descending order of utility, and accepts the front N_r units. Then, other units are rejected.

5) *End of the algorithm:* All SCs update the optimal matching Φ^* based on preference relations until convergence.

At initialization, (19) is used to consider links with average quality to reduce co-channel interference. Then, in the matching process, if there exist LEO satellites that have already been matched but cause excessive interference to GEO-GS, it is removed from the matching set \mathcal{T} . The matching process will be re-executed based on the utility to obtain the optimal matching Φ^* .

The algorithm for interference management combined with inter-satellite handover (IMISH) is shown in Algorithm 1.

Algorithm 1 Interference Management combined with Inter-Satellite Handover (IMISH)

Input: Sets of TBSs, LEO satellites and SCs \mathcal{M} , \mathcal{L} and \mathcal{K} ; interference threshold of GEO-GS I_{th} .

Output: The stable matching Φ^* .

```

1: Initialization
2: Record the current matching as  $\Phi$ . Construct  $\mathcal{M}_{un} = \mathcal{M}$  and  $\mathcal{N}_{un,k} = \mathcal{N}$ .
3: while there exists a unmatched SC  $k$  do
4:   Each unmatched SC  $k$  makes a proposal to its most preferred TBS-satellite unit  $(m, n)$  according to (19).
5:   if the unit  $(m, n)$  receives proposals from more than  $N_r$  SCs then
6:     The  $(m, n)$  accepts the first  $N_r$  SCs in utility ranking and rejects the others.
7:   else
8:     The  $(m, n)$  and  $k$  form a new matching pair.
9:   end if
10:  The TBS  $m$  is removed from  $\mathcal{M}_{un}$ .
11: end while
12: Matching Process
13: while  $\mathcal{M}_{un}$  is not  $\emptyset$  or at least one satellite-SC unit  $(l, k)$  tries to propose do
14:   Set  $\mathcal{T} = \emptyset$ .
15:   for each SC  $k$  do
16:     for each matched satellite-SC unit  $(n, k)$  do
17:       The unit  $(n, k)$  makes a proposal to its most preferred pair  $(m', (n', k))$  according to (20) and (21).
18:       Add the candidate pairs to  $\mathcal{T}$ .
19:       Calculate the interference of the GEO-GS according to (9).
20:     Handover Process
21:     while  $I \leq I_{th}$  do
22:       Rank the LEO satellites in order of interference strength and remove the most interfering one.
23:       Select the candidate pairs with the highest utility that meet the handover threshold  $H$ .
24:       Update the candidate pairs in  $\mathcal{T}$ .
25:     end while
26:   end for
27: end for
28:   for each proposed TBS  $m$  do
29:     Repeat step 6-8.
30:   The matched LEO satellites are removed from  $\mathcal{N}_{un,k}$ .
31: end for
32: end while
33: return the final matching  $\Phi^*$ .

```

B. User Association and Resource Allocation

For P2, the backhaul capacity constraint is omitted to broaden the scope of user association, thus ensuring a global optimization solution. To coordinate intra-system co-channel interference, we formulate the terrestrial resource allocation problem as a one-to-one matching. Specifically, user association and SC allocation are performed based on user distribution and channel conditions. After the optimal matching is obtained, the downlink sum rate is improved through power allocation. The algorithm is described as follows.

1) *Preparation process*: Define η is the mapping between \mathcal{J} and $\mathcal{M} \times \mathcal{C}$. We use (m, c) to represent the TBS-SC unit. The goal of a matching η is to obtain a stable $(j, (m, c))$ matching pair that maximizes the downlink sum rate.

2) *Preference relationship*: There is a dependence among SCs due to co-channel interference [26]. Specifically, the transmission rate achieved on SC c will be affected by other matched SCs. Given a SC c , it expects to form a pair $(j, (m, c))$ with a high channel gain GU j -TBS m link and a low interference GU j -TBS m' link for higher transmission rate. Therefore, a preference matrix Θ is defined to evaluate the effect on the TBS-SC unit (m, c) of all potential matching pairs as

$$\Theta_{j,(m,c)}^{j',(m',c)} = (h_{m',j',c})^\rho / (h_{m,j',c}), \quad (25)$$

where ρ is the preference parameter. Then, if $\Theta_{j_1,(m_1,c)}^{j_1,(m_1,c)} > \Theta_{j_2,(m_2,c)}^{j_2,(m_2,c)}$, the matched pair is more likely to be updated as $(j_1, (m_1, c))$ rather than $(j_2, (m_2, c))$. When $\rho = 0$, the unit is concerned with the impact of co-channel interference in matching process. When $\rho = 1$, the unit comprehensively considers the gain and co-channel interference brought by new matching pairs.

3) *Matching process*: Initially, each SC c proposes to its most preferred TBS m and GU j , satisfying $a_{m,j} = 1$. This process can be formulated as

$$(j^*, m^*) = \arg \max_{j \in \mathcal{J}_{un}, 0 \leq m \leq N_M} h_{m,j,c}, \quad (26)$$

where \mathcal{J}_{un} is the set of unmatched GUs.

According to the corresponding relationship between file requests and TBSs cache, GUs are divided into local-UEs directly served by TBSs and backhaul-GUs served by LEO satellites. Then, each TBS-SC unit (m, c) proposes to its most preferred matching pair, which satisfies

$$(j', m'_l) = \arg \max_{j'_l \in \mathcal{J}_{un}^l, m \in \mathcal{M}_{un,c}} \Theta_{j,(m,c)}^{j'_l,(m',c)}, \quad (27)$$

$$(j', m'_b) = \arg \max_{j'_b \in \mathcal{J}_{un}^b, m \in \mathcal{M}_{un,c}} \Theta_{j,(m,c)}^{j'_b,(m',c)}, \quad (28)$$

where \mathcal{J}_{un}^l and \mathcal{J}_{un}^b represent the sets of unmatched local-GUs and backhaul-GUs and $\mathcal{M}_{un,c}$ represents the set of unmatched TBSs over SC k . Sets of local and backhaul candidate pairs \mathcal{S}_c^l and \mathcal{S}_c^b consisting of $(j'_l, (m', c))$ and $(j'_b, (m', c))$ are constructed for each SC k , respectively. The utility of SC k is defined as

$$R_c^l = \sum_{m=1}^{N_M} \sum_{j=1}^{N_J} R_{m,j,c}. \quad (29)$$

Then, each SC k proposes to a candidate matching pair $(j''_l, (m'', c))$ in \mathcal{S}_c^l with the highest utility. If the candidate matching pair leads to a negative system gain, it will be rejected. Instead, a new matching pair $(j''_b, (m'', c))$ is accepted based on a modified utility function, which is given by

$$R_c^b = \sum_{m=1}^{N_M} \sum_{j=1}^{N_J} R_{m,j,c} - \sum_{m=1}^{N_M} \lambda_m \sum_{j=1}^{N_J} x_{m,j,c} (1 - g_{m,j}) U_{\text{back}}. \quad (30)$$

Accordingly, the matching rules is defined as

$$\eta_1 \succ_c \eta_2 \Leftrightarrow R_c(\eta_1) >_c R_c(\eta_2), \quad (31)$$

where $R_c(\eta)$ represents the utility obtained by SC c under η . In addition, if GU j receives multiple proposals, it only accepts the one with the highest utility and others will be rejected.

4) *Power allocation*: After the SCs and GUs are matched, fine-grained power allocation is implemented for each SC using the water injection algorithm. When performing power allocation on the SCs in the TBS, we consider the co-channel interference brought by other TBSs to remain unchanged. Therefore, the power allocation of each TBS can be optimized in a distributed manner through the water injection power algorithm. The specific details of the algorithm are not discussed as the focus. The power allocation aims at maximizing the system sum rate, achieved by distributing the power proportionately to the channel gain. Specifically, SCs with higher channel gain are allocated more power. The optimization problem for power allocation is formulated as:

$$\max_{\{P\}} \sum_{m=1}^{N_M} \sum_{j=1}^{N_J} \sum_{c=1}^{N_C} \log_2 \left(1 + \frac{x_{m,j,c} p_{m,j,c} |h_{m,j,c}|^2}{I_{m,j,c} + \sigma_n^2} \right), \quad (32)$$

Algorithm 2 User Association and Resource Allocation (UARA)

Input: Sets of TBSs, GUs and SCs \mathcal{M} , \mathcal{J} and \mathcal{C} ; association matrix A .

Output: The stable matching η^* and power allocation matrix P .

```
1: Initialization
2: Record the current matching as  $\eta$ . Construct  $\mathcal{M}_{un,c} = \mathcal{M}$ ,  $\mathcal{J}_{un} = \mathcal{J}$ ,  $\mathcal{J}_{un}^{local} = \mathcal{J}^{local}$  and  $\mathcal{J}_{un}^{back} = \mathcal{J}^{back}$ .
3: while there exists an unmatched SC  $c$  do
4:   Each unmatched SC  $c$  makes a proposal to the most preferred GU-TBS unit  $(j, m)$  according to (26).
5:   if GU  $j$  receives proposals from more than one SC then
6:     The GU  $j$  accepts the first unit in channel gain ranking and rejects the others.
7:   else
8:     The GU  $j$  and  $(m, c)$  form a new matching pair.
9:   end if
10:  The GU  $j$  is removed from  $\mathcal{J}_{un}$ .
11: end while
12: Matching Process
13: while  $\mathcal{J}_{un}$  is not  $\emptyset$  or at least one TBS-SC unit  $(m, c)$  tries to propose do
14:   Set  $\mathcal{S}_c^l = \mathcal{S}_c^b = \emptyset$ .
15:   for each SC  $c$  do
16:     for each matched TBS-SC unit  $(m, c)$  do
17:       The unit  $(m, c)$  proposes to the most preferred pair  $(j_l'', (m'', c))$  or  $(j_b'', (m'', c))$  according to (27) and (28).
18:     end for
19:   end for
20:   for each proposed GU  $j$  do
21:     Repeat step 6-8. The matched local-GUs and backhaul-GUs are removed from  $\mathcal{J}_{un}^l$  and  $\mathcal{J}_{un}^b$ .
22:     The matched TBS  $m$  is removed from  $\mathcal{M}_{un,c}$ .
23:   end for
24: end while
25: for each matched UE-TBS-SC unit do
26:   Update  $P$  with  $p_{m,j,c}$  by solving problem (32) with water injection power algorithm.
27: end for
28: return the final pair  $\eta^*$  and power allocation matrix  $P$ .
```

where N_M denotes the GUs associated with TBS m and $I_{m,j,c}$ is the intra-system co-channel interference.

5) *End of the algorithm:* All SCs update the optimal matching pairs η^* based on preference relations until convergence. The algorithm for user association and resource allocation (UARA) is shown in Algorithm 2.

C. Coordinated Intra- and Inter-system Interference Management Algorithm

The coordinated intra- and inter-system interference management (CIIM) algorithm is designed to solve the intra- and inter-system interference management problem. The proposed algorithm employs a many-to-one game-matching approach involving SCs, TBSs, and LEO satellites, while also avoiding collinear interference by inter-satellite handover. Additionally, user association and SC allocation is conducted through one-to-one matching of GUs, SCs and TBSs, and intra-system co-channel interference is further managed through power allocation. The specific steps are as follows:

- 1) Given $\lambda^{(t)}$, satellite interference management and terrestrial resource allocation subproblems are solved.
- 2) To satisfy the backhaul link constraint, if the backhaul traffic consumed by the backhaul-GUs exceeds the backhaul capacity of the TBS, the matching relationship will be removed according to transmission rate of GUs¹.
- 3) Update the λ by gradient descent formula, which is expressed as $\lambda_m^{(t+1)} = \lambda_m^{(t)} - \theta^{(t)} \left(C_m - \sum_{j=1}^{N_j} \sum_{c=1}^{N_c} x_{m,j,c} (1 - g_{m,j}) U_{back} \right)$, $\forall m \in \mathcal{M}$, where $\theta^{(t)}$ denotes the monotonically decreasing exponential function in the t -th iteration. The convergence criterion is $|\theta^{(t+1)} - \theta^{(t)}| \leq 10^{-6}$. Finally, the solution of intra- and inter-system interference management problem is obtained.

The whole algorithm is shown in detail in Algorithm 3.

D. Convergence and Computational Complexity

In this section, the convergence and computational complexity of the proposed algorithms are analyzed.

- 1) *Convergence Analysis.* The convergence of algorithms mainly depends on the matching process. The algorithm iteration stops when a stable matching is reached. In each iteration, a preliminary match is made, and then the matched units propose to the unmatched units according to the preference relation. When there is no matching element in the preference matrix of each matching element, it means that a stable matching has been achieved, and then the iteration stops.

¹Note that the original problem is an integer programming problem and the results obtained by the proposed method cannot always satisfy the constraints [30].

Algorithm 3 Coordinated Intra- and Inter-system Interference Management

```
1: Initialize  $X, B, P, \lambda$  and  $\theta^{(t)}$ .
2: while  $|\theta^{(t+1)} - \theta^{(t)}| \leq 10^{-6}$  do
3:   Solve the satellite interference management problem and update  $B$  with  $b_{l,m,k}$  by Algorithm 1.
4:   Solve the terrestrial resource allocation problem and update  $X$  with  $x_{m,j,c}$  and  $P$  with  $p_{m,j,c}$  by Algorithm 2.
5:   for each TBS  $m$  do
6:     The accessed backhaul-GUs are removed sequentially until (11g) is satisfied.
7:   end for
8:   Update  $\lambda$  and  $\theta^{(t)}$ .
9: end while
10: return  $X, B$  and  $P$ .
```

Table II
SIMULATION PARAMETERS

Parameter	Value
C-band carrier frequency f_C	4.9GHz
Ka-band carrier frequency f_{Ka}	30GHz
C-band carrier bandwidth B_C	100MHz
Ka-band carrier bandwidth B_{Ka}	500MHz
TBS transmit power	47dBm
LEO Satellite transmit power	48dBm
GEO Satellite transmit power	60dBm
G/T parameter of each TBS and satellite	18.5dB/K
Elevation angle of TBS	30°
AWGN σ_n^2	-174dBm/Hz
Preference parameters ρ	1

2) *Computational Complexity Analysis.* In IMISH algorithm, only one TBS will be matched in each iteration when no handover occurs. Thus, the number of iterations is N_M . If each SC accepts a proposal in each iteration and N_K matched units is generated, the number of iterations is $\lceil N_M/N_K \rceil$. Therefore, the iteration number is between $\lceil N_M/N_K \rceil$ and N_M . Furthermore, if the number of LEO satellites connected to a TBS m does not exceed N_T , each matched TBS-satellite unit (m,l) will construct a preference matrix with a size of $N_M \times N_L$. Consequently, the complexity is $O(N_M^3 \times N_L \times N_K)$ without handover. When the inter-satellite handover is required, the worst case is that all LEO satellites need to be removed and the handover utility of each LEO satellite needs to be calculated. Accordingly, the complexity of IMISH algorithm is $O(N_M^3 \times N_L^2 \times N_K)$. Similarly, the iteration number of UARA algorithm is between $\lceil N_J/N_C \rceil$ and N_J . Then, power allocation needs to be implemented on each SC c . Thus, the complexity of UARA is $O(N_T^3 \times N_G \times N_C^2 + N_T \times N_G \times N_C)$. Therefore, the complexity of CIIM is $O((N_M^3 \times N_J \times N_C^2 + N_M \times N_J \times N_C) \times i_{max})$ considering $N_L \ll N_J$ in ISTN, where i_{max} indicates the iteration numbers.

V. SIMULATION RESULTS

The simulation scene is a 3 km \times 3 km area, where the GUs and TBSs are subject to random distribution and uniform distribution in the coverage of the satellites, respectively. The GEO and LEO satellites provide service to TBSs, and the LEO satellite uses the actual trajectory data from LEO satellites in the SpaceX constellations. The file caching strategy of TBS adopts random scheme (RS) [31]. And the Zipf distribution index ω is set to 0.5. The total number of the popular files in the terrestrial network is 50 and 40 files are cached by the TBS. The terrestrial network adopts 5G communication system, which has 273 resource blocks (RBs). And each LEO satellite has 8 SCs. The total simulation time is 24 hours, divided into 1440 time slots. The channel between TBSs and GUs and the channel between LEO satellites and TBSs are modeled as Rayleigh fading and Rician fading, respectively. Other simulation parameters are set according to [32], as shown in Table II.

A. Benchmark Algorithms

In this section, we compare the proposed algorithm with existing algorithms to evaluate the performance. For satellite interference management and inter-satellite handover, five algorithms are given:

- **Joint interference management and user association (JIMUA) algorithm:** As the description in [33], interference management is addressed through collaborative computing. This method ignores the impact of inter-satellite handover on interference management. The complexity is $O(N_T^3 \times N_G \times N_C \times i_{max})$.
- **Minimum distance handover (MDH) algorithm:** In this algorithm, minimum distance inter-satellite handover is introduced. The TBS will switch from the LEO satellite connected in the current time slot to the nearest LEO satellite.

Table III
COMPARED WITH ES

N_M	N_J, N_C	Time (s), Rate (Mbps)	
		ES	UARA
2	4, 2	0.030797, 19.3615	0.000668, 19.3615
	5, 2	0.262131, 21.2870	0.000737, 21.2870
	6, 2	0.578923, 22.4408	0.001158, 22.4402
	6, 3	76.30533, 32.1752	0.003353, 32.1752
	7, 3	1187.87395, 33.7628	0.015913, 33.7609

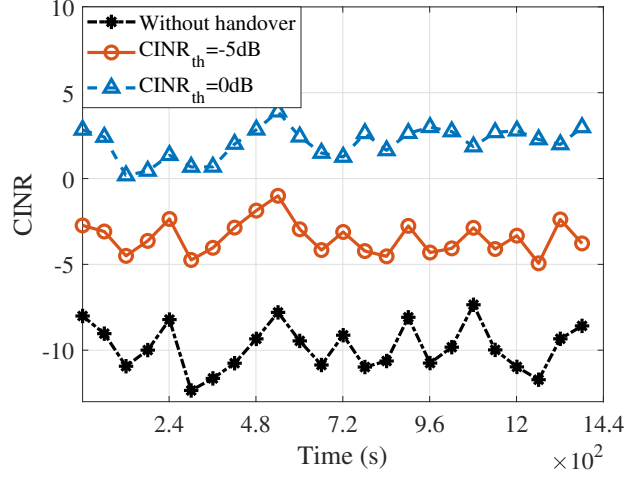


Fig. 2. CINR of GEO-GS versus time under different working thresholds.

- **Random resource allocation and inter-satellite handover management (RRAIHM) algorithm:** In this algorithm, LEO satellites randomly allocate SCs to TBSs and other steps are similar to IMISH.
- **Greedy algorithm:** In this algorithm, LEO satellite SCs are allocated to TBSs, which can achieve the highest backhaul rate.
- **Random algorithm:** In this algorithm, LEO satellite SCs are randomly allocated to TBSs.

For terrestrial resource allocation, two algorithms are given:

- **Exhaustive search (ES) algorithm:** In ES algorithm, the optimal solution is obtained by exhaustively enumerating all possible matching combinations. The complexity is $O(N_J^{N_M \times N_C})$.
- **User association and average allocation (UAAA) algorithm:** In UAAA algorithm, TBSs equally distributes the power to each SCs and other steps are similar to UARA.

B. Comparison with Benchmark Algorithms

A small-scale test is conducted to evaluate the gap between UARA and ES. Table III shows the performance comparison of UARA and ES for varying numbers of GUs and SCs. It is evident that the computation time of ES increases rapidly as N_J and N_C increase. Meanwhile, when $N_J > N_M \times N_C$, UARA can significantly save computation time while maintaining a <1% loss compared to ES.

Fig. 2 illustrates the CINR of GEO-GS versus time under different working thresholds. It can be found that inter-satellite handover can effectively improve the CINR of the GEO-GS, leading to an improvement of over 6.4 dB compared to the situation without handover. The reason is that CIIM removes specific interference from LEO satellites during the handover process. However, inter-satellite handover would also degrade the backhaul capability, resulting in a decline in the sum rate. Fig. 3 shows how handover affects the system sum rate. We can observe that as the working threshold increases, the system sum rate will decrease. This can be attributed that as the working threshold increases, the LEO satellites can be connected by TBSs reduces. When user density D_{GU} is high, excessive handovers lead to a loss of 7.5% of the sum rate. Accordingly, $CINR_{th}=0dB$ is adopted as a benchmark in the following simulations.

Figs. 4 and 5 depict the impact of handover threshold H on the LEO backhaul capacity and average handover times. It can be seen that when the handover threshold H increases, the backhaul capacity achieved by IMISH and RRAIHM will first increase and then decrease. This is because a small handover threshold is beneficial to handover triggering, resulting in

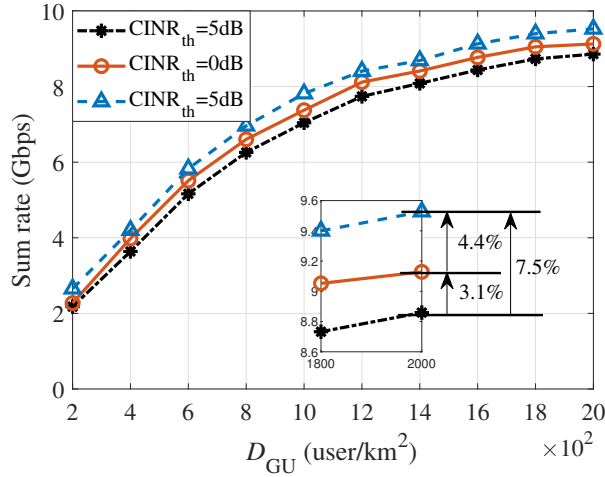


Fig. 3. System sum rate versus user density D_{GU} under different $CINR_{th}$.

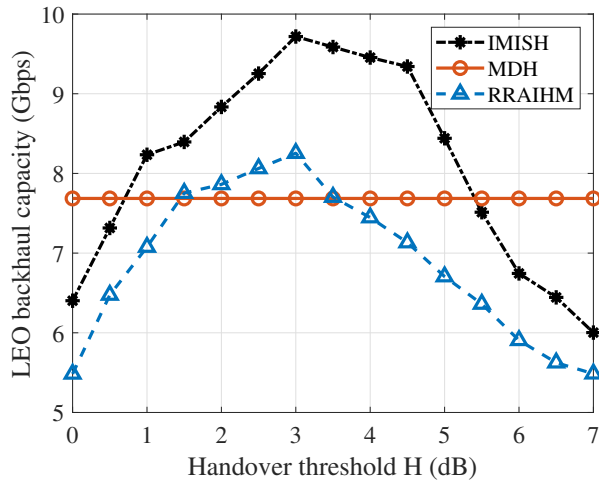


Fig. 4. LEO backhaul capacity versus handover thresholds under different schemes.

a significant increase in backhaul capacity. Especially, when the handover threshold exceeds 3dB, the increase in handover threshold greatly limits the improvement of backhaul capacity. Meanwhile, the increase in handover threshold reduces the LEO satellites that meet the handover conditions, which leads to a decrease in handover times. Since the handover criterion adopted by MDH is the minimum distance, the change of handover threshold does not affect its performance. In addition, the average handover times of IMISH are always lower than other algorithms. The reason is that during the matching process, the setting of the utility function considers the influence of inter-satellite interference, so excessive handover is not required. It is also noticed that compared with RRAIHM and MDH, the backhaul capacity obtained by IMISH is increased by 17.7% and 29.8%, respectively. The reason is that TBS selects LEO satellites with higher gain and less interference, thereby reducing inter-satellite interference. To balance the handover times and backhaul capacity, $H=3\text{dB}$ is used as a benchmark in subsequent simulations.

In the context of combining UARA with the upper bound and UA, Fig. 6 illustrates the performance comparison of downlink sum rate as the user density increases under various algorithms. The ideal backhaul is set for each TBS, so that the achieved sum rate is considered as the upper bound. The results reveal that the sum rate increases with D_{GU} . The reason is that the gain brought by user access is more obvious than the impact of increased interference. Compared with the upper bound, the lower backhaul capacity achieved by CIIM results in a reduced sum rate. Compared with UA, UARA performs power allocation according to user distribution and channel conditions, thereby improving the sum rate. It is noteworthy that the gap between the results obtained by UARA and the upper bound is reduced as the user density increases, with only a 3.1% loss at $U_{\text{back}}=3\text{Mbps}$, which shows that UARA can effectively increase the transmission rate through using decomposition and addressing the original

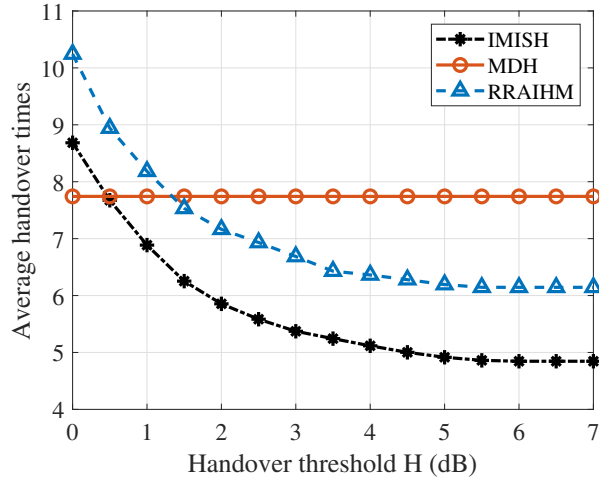


Fig. 5. Average handover times versus handover thresholds under different schemes.

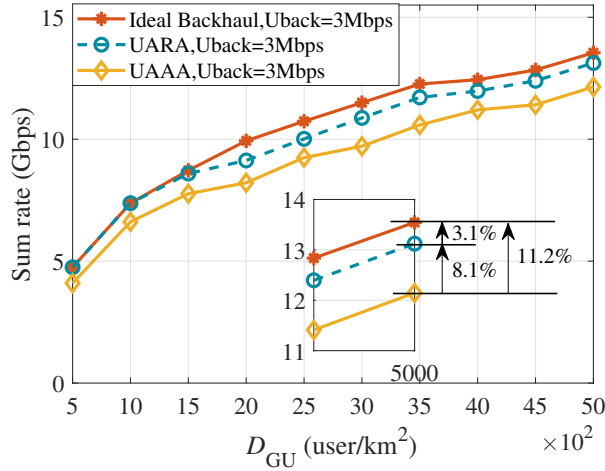


Fig. 6. System sum rate versus user density D_{GU} under different schemes ($U_{back}=3\text{Mbps}$).

problem simultaneously.

C. Performance of IMISH in Different Constellations

We simulate the performance of IMISH under different N_r and constellations to show its effectiveness for capacity improvement. Fig. 7 simulates the backhaul capacity under different algorithms when the number of connected satellites N_r changes. As N_r increases, the LEO backhaul capacity achieved by different algorithms initially increases and then approaches saturation. When $N_r=3$, the effect of the multi-connection feature on the improvement of the LEO backhaul capacity reaches saturation. This is because the co-channel interference caused by multiple connections between LEO satellites and TBSs limits the gain, so that the obtained backhaul capacity remains stable.

To further explore the situation of algorithm performance under different numbers of satellites, we set up four satellite constellations. Each type consists of 36 orbital planes with 40, 55, 75, and 100 LEO satellites in each plane. Fig. 8 illustrates the backhaul capacity obtained by different algorithms in different scale constellations. It reveals that the backhaul capacity obtained by CIIM is always better than that of JIMUA and keeps increasing as the size of the constellation increases, while the other two algorithms are insensitive to the changes in the number of satellites. This is because the IMISH considers the impact of interference on link quality and improve the backhaul capacity by inter-satellite handover. As the scale of the constellation continues to increase, it is necessary to effectively manage the interference within the constellation to increase the backhaul capacity.

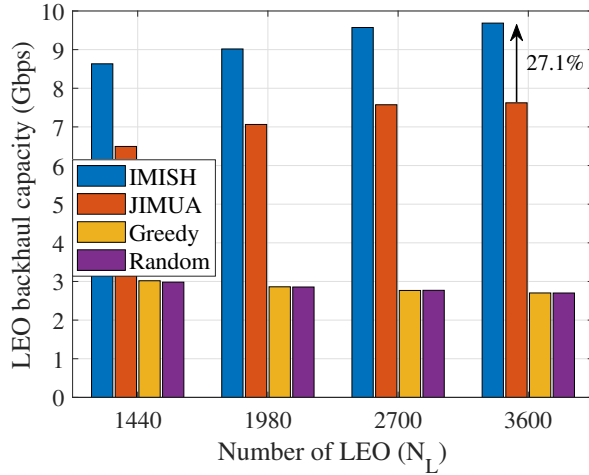


Fig. 7. Comparison of LEO backhaul capacity with different N_r under different schemes ($H = 3\text{dB}$ and $CINR_{th} = 0\text{dB}$).

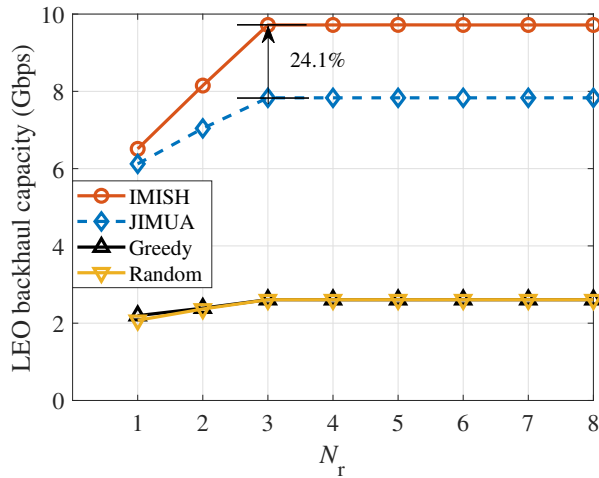


Fig. 8. Comparison of LEO backhaul capacity with different N_L under different schemes ($H = 3\text{dB}$ and $CINR_{th} = 0\text{dB}$).

VI. CONCLUSION

In this paper, we investigate the coordinated design of intra- and inter-system interference management and interference avoidance through inter-satellite handover in ISTN. In particular, a coordinated intra- and inter-system interference management (CIIM) scheme is proposed to coordinate intra-system co-channel interference while satisfying the constraint of inter-system interference. Through inter-satellite handover, TBS can make handover decisions to avoid collinear interference between GEO and LEO satellites. In addition, we propose a user association and resource allocation scheme to conduct the user association and coordinate the co-channel interference among GUs. The simulation results show the effectiveness of CIIM in mitigating inter-system collinear interference and improving the downlink sum rate of ISTN. Hence, this study can offer the reference for overcoming the intra- and inter-system interference in ISTNs.

REFERENCES

- [1] D. Zhou, M. Sheng, J. Li, and Z. Han, "Aerospace integrated networks innovation for empowering 6G: A survey and future challenges," *IEEE Commun. Surv. Tut.*, vol. 25, no. 2, pp. 975–1019, Feb. 2023.
- [2] M. Sheng, D. Zhou, W. Bai, J. Liu, and J. Li, "6G service coverage with mega satellite constellations," *China Commun.*, vol. 19, no. 1, pp. 64–76, Jan. 2022.
- [3] M. Sheng, D. Zhou, R. Liu, Y. Wang, and J. Li, "Resource mobility in space information networks: Opportunities, challenges, and approaches," *IEEE Netw.*, vol. 33, no. 1, pp. 128–135, Jan. 2019.
- [4] S. Chen, S. Sun, and S. Kang, "System integration of terrestrial mobile communication and satellite communication —the trends, challenges and key technologies in B5G and 6G," *China Commun.*, vol. 17, no. 12, pp. 156–171, Dec. 2020.

- [5] X. S. Shen, N. Cheng, H. Zhou, L. Feng, W. Quan, W. Shi, W. U. Huaqing, C. Zhou, X. University, and N. University, "Space-air-ground integrated networks: review and prospect," *Chinese J. Int.*, vol. 4, no. 3, pp. 3–19, Sep. 2020.
- [6] D. Zhou, M. Sheng, J. Luo, R. Liu, J. Li, and Z. Han, "Collaborative data scheduling with joint forward and backward induction in small satellite networks," *IEEE Trans. Commun.*, vol. 67, no. 5, pp. 3443–3456, May. 2019.
- [7] A. Destounis and A. D. Panagopoulos, "Dynamic power allocation for broadband multi-beam satellite communication networks," *IEEE Commun. Lett.*, vol. 15, no. 4, pp. 380–382, Apr. 2011.
- [8] K. Nakahira, K. Kobayashi, and M. Ueba, "Capacity and quality enhancement using an adaptive resource allocation for multi-beam mobile satellite communication systems," in *Proc. Wireless Commun. Netw. Conf.*, Las Vegas, NV, Apr. 2006, pp. 153–158.
- [9] U. Park, H. W. Kim, D. S. Oh, and D. I. Chang, "Performance analysis of dynamic resource allocation for interference mitigation in integrated satellite and terrestrial systems," in *Proc. Int. Conf. Next Gener. Mobile Appl.*, Cambridge, United Kingdom, Sep. 2016, pp. 217–221.
- [10] Y. Zhang, H. Zhang, H. Zhou, K. Long, and G. K. Karagiannidis, "Resource allocation in terrestrial-satellite-based next generation multiple access networks with interference cooperation," *IEEE J. Sel. Areas in Commun.*, vol. 40, no. 4, pp. 1210–1221, Apr. 2022.
- [11] R. Liu, M. Sheng, K.-S. Lui, X. Wang, Y. Wang, and D. Zhou, "An analytical framework for resource-limited small satellite networks," *IEEE Commun. Lett.*, vol. 20, no. 2, pp. 388–391, Feb. 2016.
- [12] S. K. Sharma, S. Chatzinotas, and B. Ottersten, "Inline interference mitigation techniques for spectral coexistence of GEO and N GEO satellites," *Int. J. Satell. Commun. Netw.*, vol. 34, no. 1, pp. 11–39, Sep. 2014.
- [13] A. Pourmoghadas, S. K. Sharma, S. Chatzinotas, and B. Ottersten, "Cognitive interference management techniques for the spectral co-existence of GSO and N GEO satellites," in *Proc. Int. Conf. Wireless Satell. Syst.*, Genova, Italy, Jul. 2016, pp. 178–190.
- [14] P. Xu, C. Wang, J. Yuan, Y. Zhao, and W. Wang, "Uplink interference analysis between LEO and GEO systems in ka band," in *Proc. 2018 IEEE 4th Int. Conf. Comp. Commun.*, Chengdu, China, Dec. 2018, pp. 789–794.
- [15] W. Hui, C. Wang, J. Yuan, Y. Zhao, and W. Wang, "Coexistence downlink interference analysis between LEO and GEO systems in ka band," in *Proc. 2018 IEEE 4th Int. Conf. Comp. Commun.*, Chengdu, China, Dec. 2018, pp. 465–469.
- [16] R. Li, P. Gu, and C. Hua, "Optimal beam power control for co-existing multibeam GEO and LEO satellite system," in *Proc. 2019 11th Int. Conf. Wireless Commun. and Signal Process.*, Xi'an, China, Oct. 2019, pp. 1–6.
- [17] S. Chen, Y.-C. Liang, S. Sun, S. Kang, W. Cheng, and M. Peng, "Vision, requirements, and technology trend of 6G: How to tackle the challenges of system coverage, capacity, user data-rate and movement speed," *IEEE Wireless Commun.*, vol. 27, no. 2, pp. 218–228, Apr. 2020.
- [18] Z. Wu, F. Jin, J. Luo, Y. Fu, J. Shan, and G. Hu, "A graph-based satellite handover framework for LEO satellite communication networks," *IEEE Commun. Lett.*, vol. 20, no. 8, pp. 1547–1550, Aug. 2016.
- [19] K. Zhu, C. Hua, P. Gu, and W. Xu, "User clustering and proactive group handover scheduling in LEO satellite networks," in *Proc. 2020 IEEE Comp., Commun. IoT Appl.*, Beijing, China, Dec. 2020, pp. 1–6.
- [20] L. Feng, Y. Liu, L. Wu, Z. Zhang, and J. Dang, "A satellite handover strategy based on MIMO technology in LEO satellite networks," *IEEE Commun. Lett.*, vol. 24, no. 7, pp. 1505–1509, Jul. 2020.
- [21] S. Ni, J. Liu, M. Sheng, J. Li, and X. Zhao, "Joint optimization of user association and resource allocation in cache-enabled terrestrial-satellite integrating network," *Sci. China Inf. Sci.*, vol. 64, no. 8, pp. 1–14, Jun. 2021.
- [22] L. Wang, Y. Wu, H. Zhang, S. Choi, and V. Leung, "Resource allocation for NOMA based space-terrestrial satellite networks," *IEEE Trans. Wireless Commun.*, vol. 20, no. 2, pp. 1065–1075, Feb. 2021.
- [23] F. Pervez, L. Zhao, and C. Yang, "Joint user association, power optimization and trajectory control in an integrated satellite-aerial-terrestrial network," *IEEE Trans. Wireless Commun.*, vol. 21, no. 5, pp. 3279–3290, May 2022.
- [24] W. Qiu, A. Liu, C. Han, and L. U. Aihong, "Joint user association and spectrum allocation in satellite-terrestrial integrated networks," *IEICE Trans. Commun.*, vol. E105-B, pp. 1063–1077, Sep. 2022.
- [25] T. Leng, P. Duan, D. Hu, G. Cui, and W. Wang, "Cooperative user association and resource allocation for task offloading in hybrid GEO-LEO satellite networks," *Int. J. Satell. Commun. Netw.*, vol. 40, no. 3, pp. 230–243, May. 2022.
- [26] B. Di, H. Zhang, L. Song, Y. Li, and G. Y. Li, "Ultra-dense leo: Integrating terrestrial-satellite networks into 5G and beyond for data offloading," *IEEE Trans. Wireless Commun.*, vol. 18, no. 1, pp. 47–62, Jan. 2019.
- [27] M. Zink, K. Suh, Y. Gu, and J. Kurose, "Characteristics of youtube network traffic at a campus network – measurements, models, and implications," *Comp. Netw.*, vol. 53, no. 4, pp. 501–514, Sep. 2009.
- [28] J. Zhang, L. Xiang, D. W. K. Ng, M. Jo, and M. Chen, "Energy efficiency evaluation of multi-tier cellular uplink transmission under maximum power constraint," *IEEE Trans. Wireless Commun.*, vol. 16, no. 11, pp. 7092–7107, Nov. 2017.
- [29] Y. Tang, P. Yang, W. Wu, J. W. Mark, and X. Shen, "Interference mitigation via cross-tier cooperation in heterogeneous cloud radio access networks," *IEEE Trans. Cogn. Commun. Netw.*, vol. 6, no. 1, pp. 201–213, Mar. 2020.
- [30] S. Boyd and L. Vandenberghe, "Convex optimization: Theory," 2004.
- [31] S. Chen, W. Ye, Y. Jia, N. Wang, and Y. Yan, "User association in cache-enabled ultra dense network with JT CoMP," in *Proc. 2018 IEEE 3rd Adv. Inf. Technol. Electron. Automat. Control Conf.*, Chongqing, China, Oct 2018, pp. 964–968.
- [32] J. Yli-Kaakinen, T. Levanen, A. Palin, M. Renfors, and M. Valkama, "Generalized fast-convolution-based filtered-ofdm: Techniques and application to 5G new radio," *IEEE Trans. Signal Process.*, vol. 68, p. 1213–1228, Feb. 2020.
- [33] L. Zhang, J. Liu, M. Sheng, N. Zhao, and J. Li, "Exploiting collaborative computing to improve downlink sum rate in satellite integrated terrestrial networks," *IEEE Trans. Veh. Technol.*, vol. 72, no. 4, pp. 4670–4682, Apr. 2023.